



## The Effect of Butyl Glycol Acetate/Ethyl Acetate Mixed Solvents Composition on Nitrocellulose Solution Emulsification: The Stability of Resultant Colloid and Micro-filterability

Halimeh Javidnia<sup>1</sup>, Naser Mohammadi<sup>1\*</sup>, Ahmad Mousavi Shooshtari<sup>2</sup>, Somayeh Ghasemirad<sup>1</sup>, Tohid Farajpoor<sup>3</sup>, and Mohammad Reza Ghanbari<sup>1</sup>

(1) Loghman Fundamental Research Group, Department of Polymer Engineering and Color Technology, Amirkabir University of Technology,

P.O. Box: 15914-4413, Tehran, Iran

(2) Textile Engineering Department, Amirkabir University of Technology,

P.O. Box: 15875-4413, Tehran, Iran

(3) Chemistry Group, Amirkabir University of Technology,

P.O. Box: 15875-4413, Tehran, Iran

Received 3 January 2009; accepted 17 April 2010

### ABSTRACT

The effect of butyl glycol acetate (BGA)/ethyl acetate (EA) mixed solvents composition on nitrocellulose (NC) solution miscibility and rheological properties with or without non-ionic surfactants was investigated. In addition the emulsification of the solution containing two non-ionic surfactants with weight average hydrophilic/lipophilic balance of 14.75 (oil phase), its colloidal stability and micro-filterability were studied. The results showed that oil phase viscosity and surface tension increase by high boiling point solvent (BGA) between 50 and 87.5 wt%, which reduced the colloid particle size from 35  $\mu\text{m}$  down to 10  $\mu\text{m}$ . While surfactant free solution viscosity of NC in the BGA/EA mixed solvents increased to a maximum at 75 wt% of BGA, the addition of the non-ionic surfactants changed the situation to a minimum at the same BGA content. The complex behaviour was assigned to the competitive interactions of solution components via hydrogen bond formation. The colloid particle size decreases depended also on  $\Delta g_{\text{mix}}^c$ , the Gibbs free energy density of mixing two phases, due to higher solution BGA content. Power law dependence of 0.09 and -1.31 was found for the colloid particle size or sedimentation rate dependence on  $\Delta g_{\text{mix}}^c$  and the oil phase viscosity, respectively. Finally, the prepared colloidal systems did not permeate through the membrane with 400 nm cross-through channels under 10 atm of nitrogen pressure, which was attributed to the oil phase non-ionic surfactants adsorption on the membrane surfaces.

### Key Words:

emulsification;  
nitrocellulose;  
non-ionic surfactant;  
stability;  
micro-filtration.

### INTRODUCTION

Nitrocellulose (NC) thin films are of great use in different industries such as microelectronics, coatings, purifications, leather and DNA studies [1]. Polymer film formation was used to be conducted via spraying or casting of its solution on a suitable surface followed by solvent(s) vaporization. Nowadays, however, applications of organic solvents are restricted due to the environmental and economical concerns. Therefore, polymer

solutions are mainly substituted by water based colloids. Using colloidal systems, not only one can overcome the above mentioned problems, but being able to carry high solids with less viscosity. Water borne NC lacquers are used in wood coatings due to their degradability by microorganisms, transparency, good adhesion to the substrate, good mechanical strength, fast drying rate, ease of spraying, nice pigment dispersion

(\* ) To whom correspondence to be addressed.

E-mail: mohamadi@aut.ac.ir

and compatibility with most resins and plasticizers [2]. However, the colloidal state of NC is only accessible through direct emulsification [3]. In this process, oil droplets are formed within the continuous phase, water, via shearing a two-phase water/oil mixture, containing suitable surfactants [4,5]. Double and capillary break up are proposed as the governing emulsification mechanisms [6,7]. The stability of the resulting colloidal system depends mainly on density difference between the continuous and oil phases, the viscosity of continuous phase, average particle size and size distribution and particles repelling mechanisms (stabilization type and efficiency) [8-10]. In addition, oil phase compatibility with the continuous phase may play a decisive role in the colloid stability [11].

Molecular attractions and repulsions among polymer, solvent(s) and surfactants with long alkyl tails (more than 12 carbons) may induce complex formation in the oil phase leading to polymer chain stiffening [12-14]. Therefore, the oil phase behaviour depends on temperature, surfactant(s) type and content, solvent(s), solution pH and chain flexibility. Dale et al. [9] reported enhanced critical flocculation temperature for water-in-oil emulsions or their thermal stability improvement using mixture of non-ionic surfactants with different chain lengths. The phenomenon has been attributed to the constant surfactant layer thickness on particles with reduced number of attracted segments. Synergisms in interfacial layer formation among non-ionic surfactants with hydrophilic/lipophilic balance (HLB) within the range of 4.6 to 14.2 have also been reported in water-in-oil emulsions [15]. Similar synergism in the interfacial layer formation with mixed ionic and non-ionic surfactants was also reported for making oil-in-water micro-emulsions [16]. The phenomenon was assigned to the possibility of some interfacial bond formation with different strengths [15]. Dynamic surface tension of the surfactant mixture was close to the ionic surfactant characteristics (low value) while the static surface tension and critical micelle concentration were close to the non-ionic surfactant value (low value) [17].

Nakashima et al. [18] pioneered the cross-flow membrane direct emulsification while Mohammadi et

al. [5] developed the technique for dead-end direct premix membrane filtration to prepare nanoparticles. Later, Jeong et al. [19] practiced the mini-emulsification of a thermoplastic elastomer to investigate the efficacy of co-stabilizer along with three homogenization techniques: Manton-Gaulin homogenizer, sonifier and membrane filtration on the final colloid particle size distribution. Lower pressures and enhanced number of filtrations were found as the best technique to achieve narrower particle sizes. Oil phase content, however, did not alter the particle size while changed the filtration flow rate [20]. Colloidal systems with mixture of ionic and non-ionic surfactants could be ultra-filtered through amphoteric ceramic membranes in their iso-electric point [21]. In addition, NC emulsification with ionic/non-ionic surfactant mixtures or ionic surfactants was reported [3,22]. Non-ionic surfactant miscibility with the oil phase facilitates droplet break up while ionic surfactants cause its deterioration [23]. Nonetheless, non-ionic surfactants reduce permeation rate through membranes due to facilitated droplet fracture by their higher dynamic surface tension [24].

In this research work, the emulsification of NC solution, the resultant colloid stability and micro-filterability as a function of mixed BGA/EA solvent composition containing non-ionic surfactants with average HLB value of 14.75 in aqueous solution of Ultravon GPN were investigated. The sedimentation rate of the resultant colloid has been investigated by light scattering and correlated simultaneously with the  $\Delta G$  of mixing water/oil phases and the oil phase viscosity.

## EXPERIMENTAL

### Materials

Nitrocellulose (NC), with viscosity average molecular weight of 97000 g/mol containing  $11 \pm 0.5\%$  of nitrogen, and ethyl acetate (EA) were received from lacquer industries (Iran). Butyl glycol acetate (BGA), cyclohexanone, dibutyl phthalate, aqueous hydrochloric acid (37 wt%) and ammonia (25 wt%) were purchased from Merck Co. (Canada) Triton X-100, and Irgasol NA, (both with pH of 5 wt% aqueous solution = 8) were obtained from Sigma Aldrich

**Table 1.** Different oil phase recipes used for the nitrocellulose solution emulsification.

Sample Material	1-1	1-2	1-3	1-4
	Weight (g)	Weight (g)	Weight (g)	Weight (g)
Dibutyl phthalate	9	9.0	9	9.0
Nitrocellulose	36	36.0	36	36.0
Butyl glycol acetate	42	52.5	63	73.5
Ethyl acetate	42	31.5	21	10.5
Triton X-100	9	9.0	9	9.0
Irgasol NA	9	9.0	9	9.0

(Germany). Ultravon GPN ionic surfactant was received from Ciba Co (Germany).

### Direct Emulsification

NC was dried for 10 h to constant weight in laboratory to remove its processing added alcohol. Then, 36 g of the polymer was swelled for 24 h in 84 g of the mixed solvents plus 9 g of dibutyl phthalate and 18 g of equal weights of two non-ionic surfactants (Table 1). The oil phase was then mixed to a homogeneous solution in a 250 cm<sup>3</sup> beaker, 7.5 cm in diameter, by a high shear dispersing impeller, 5 cm in diameter with 10 right-angled trapezoids, 1 cm in height with 45° acute, located up and down alternatively. A mechanical mixer (Heidolph, 2102 control z) was used to rotate the impeller at 100 rpm (shear rate = 12.45 s<sup>-1</sup>). Then, 73.5 g of the oil phase was added to 300 g of deionized water containing 30 g of ammonia (pH 10) and 6 g of Ultravon GPN in a stainless steel tank, 12 cm in diameter, in 15 min. The mixture was then agitated using the dispersing impeller at 2000 rpm (shear rate = 250 s<sup>-1</sup>) in 30°C water bath for 45 min. Later, the crude latex was filtered through mono-sized polycarbonate membrane (400 nm in diameter, Advantec MFS, Inc.) under up to 10 bar of nitrogen gas pressure.

### Characterizations

#### Rheometry

The viscosity of the oil phase with and without the non-ionic surfactants was studied by a coaxial rheometer (Haake RV 12) under ascending and descending shear rates of 0-100 s<sup>-1</sup> at room temperature.

#### Tensiometry

Surface tension of the oil phase with and without the non-ionic surfactants was determined by the Wilhelmy plate method using a K14 Kruss tensiometer.

#### Optical Microscopy

A drop of emulsion was sprayed on a glass slide and immediately covered with another glass slide. Then, the sandwiched emulsion drop was observed under optical microscope (Leica VMHT MOT, Linkam, England), and photographed under magnification of 200. Picture analysis was conducted using a particle size analyzer.

#### Membrane Filtration

Polycarbonate membrane with uniform 0.4 μm in diameter channels, porosity of 0.0154 and diameter of 47 mm (Advantec MFS, Inc) was installed in standard pressure cell apparatus and used for membrane filtration under nitrogen gas pressure.

#### Turbidimetry

The rate of colloid sedimentation was measured by a home-made turbidimeter. Laser beam, 5 mW in power and wavelength of 650 nm, was passed through the dilute colloid in poly(methyl methacrylate) cuvette (Bayer, Germany), 5×5×20 mm<sup>3</sup> in length, located at 6.8 cm from the laser source, and 1.5 cm from the light detector (Lutron, LM, 81 LX).

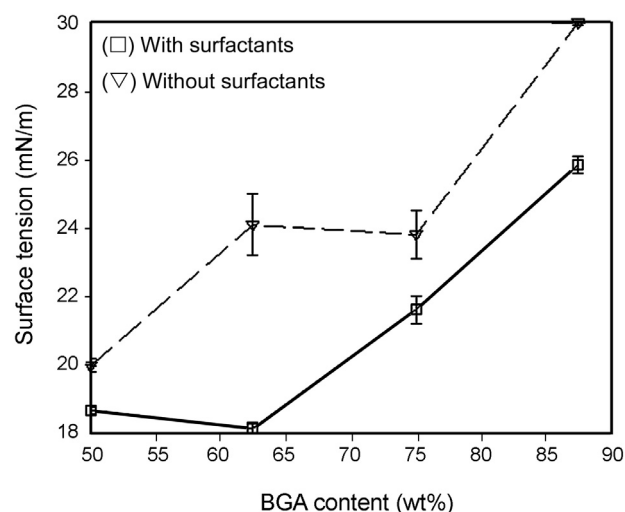
## RESULTS AND DISCUSSION

Figure 1 shows typical oil phase viscosity (samples



complexation probability among the oil phase components needs to be evaluated. The non-ionic surfactants and mixed solvents of the oil phase may form hydrogen bonds with the NC molecules via partially dissociated  $N^+$  ( $NO_2$ ) or  $H^+$  ( $OH$ ) ions leading to polymer chain stiffening (Figure 3). The increases in non-volatile solvent content may change the oil phase viscosity through several scenarios (Figure 2). On the one hand, the increased BGA content enhances the solution viscosity due to lower NC solubility leading to higher chain entanglement density. On the other hand, the increased BGA content lowers the complexation probability among the mixed solvents molecules and the NC chains, forcing their conformational transition to helices with higher entanglement density and likewise with solution viscosity. Finally, the non-volatile solvent increase may shift the oil phase to its semi-dilute or concentrated regimes,  $C^* = 0.06 \text{ g/cm}^3$  based on  $C_\infty = 10$  assumption for NC and  $C^{**} = 7C^*$ , which also increases the entanglement density of solution leading to higher oil phase viscosity. Therefore, the viscosity raise of the surfactant-free oil phase via increasing its BGA content from 62.5 wt% to 75 wt% is expectable. The viscosity reduction of the surfactant-free oil phase corresponding to the 87.5 wt% of BGA may be assigned to the forced NC/BGA molecules interactions. In other words, NC chains of this oil phase formulation are stretched to some extent due to their interactions with bigger size solvent molecules ( $v_{BGA} \approx 2v_{EA}$ ,  $v$  is the molar volume), leading to steric hindrances. Therefore, the solution entanglement density may decrease leading to viscosity drop. By adding the non-ionic surfactants to the oil phase containing 75 wt% of BGA in mixed solvents, the polymer chains are stretched due to their preferred complexation with the surfactant molecules leading to lower solution entanglement density. Further, higher BGA content of 87.5 wt%, however, may probably enhance the solution entanglement density due to the attached surfactant coiling in less favourable solvent which results in viscosity increase again.

The surface tension of the oil phase with or without surfactants was measured and plotted versus the BGA content of the mixed solvents (Figure 4). Surface tension of the surfactant-free oil phase



**Figure 4.** Surface tension of nitrocellulose solutions versus their BGA content (solid and dashed lines are for eye guidance).

containing 50 wt% of BGA in the mixed solvents was about 20 mN/m. Surface free energy of NC was about 38 mN/m which through solubilizing in the 50/50 BGA/EA mixed solvents decreased to 20 mN/m. It is well-known that the polymer content increase in solution enhances its surface tension via the following equation [25]:

$$\gamma_{\text{mix}} = \gamma_{\text{solv}} + Ae^{B\phi_{\text{solv}}} \quad (1)$$

where  $\gamma_{\text{mix}}$ ,  $\gamma_{\text{solv}}$  and  $\phi_{\text{solv}}$  are solution surface tension, solvent surface tension and solvent weight fraction, respectively, while  $A$  and  $B$  are the system constants ( $B$  is negative). The important point is that the solution concentrations are constant while the solvent quality changes by the increased BGA content of the mixed solvent. Daoud et al. [26], in their fundamental publication, showed the behavioural equivalence of lower solvent quality with the increased solution concentration. The increase to 62.5 wt% of BGA content of the mixed solvents to a surfactant-free oil phase increased the solution surface tension. Further increase in BGA content of the solution mixed solvents to 75 wt%, however, did not change the surface tension (Figure 4). The observed plateau in solution surface tension between 62.5 and 75 wt% of BGA in surfactant-free solutions could be attributed to comparable cohesiveness of

both solutions. By increasing the wt% of BGA in the mixed solvents of the NC solutions, stronger interactions may be formed while the number of interacting points may be decreased. The BGA content of 87.5 wt% increase in the mixed solvents of surfactant-free oil phase causes the partitions of the bigger BGA molecules via depletion by smaller EA molecules in favour of their interactions with NC chains leading to stronger interaction among the components and higher surface tension. Adding non-ionic surfactants to the oil phase decreased the solutions surface tensions. Nevertheless, the BGA content increase from 50 to 62.5% in the mixed solvents of the surfactant containing oil phase and subsequently to 75 and 87.5 wt%, initially lowered the system surface tension while increased it later in proportion with the BGA content of surfactant-containing oil phase. The BGA content increases to above 62.5 wt%, probably led to the increased ionic strength of the oil phase with higher surface tensions due to the long range interactions among the components mainly via the alkyl tails of the surfactants, which are more sensitive to shear forces.

The Flory-Huggins based calculations of the oil phase free energy density of mixing versus its BGA content with or without surfactants was conducted using eqn (2):

$$\Delta g_{mix} = kT \left[ \sum_{i=1}^m \frac{\phi_i \ln \phi_i}{n_i v_i} + \sum_{i=1}^m \sum_{j=i+1}^m \frac{\chi_{ij}}{v_{ij}} \phi_i \phi_j \right] \quad (2)$$

where  $\Delta g_{mix}$ ,  $n_i$ ,  $\phi_i$ ,  $v_i$ ,  $\chi_{ij}$  and  $v_{ij}$  are the excess free energy density of mixing, the components degree of polymerization, volume fraction, unit cell molar volume, pair-wise interaction parameters per unit cells and average unit cell volume of the mixture, respectively. The solubility parameters and molar volumes of the components used for the calculations are tabulated in Table 2. The oil phase free energy density of mixing ( $\Delta g_{mix}^0$ ) decreased by the non-volatile solvent content increase due to the solubility enhancement among the components (Figure 5). Addition of the non-ionic surfactants to the oil phase, however, led to the compatibility deterioration or  $\Delta g_{mix}^0$  increase. The oil phase  $\Delta g_{mix}^0$  versus its mixed solvent BGA content verified the surface tension measurements. In other words, the surface

**Table 2.** Molar volume and solubility parameter of the oil phase components.

Material	$v$ (cm <sup>3</sup> /mol)	$\delta$ (cal/cm <sup>3</sup> ) <sup>0.5</sup>
Nitrocellulose	186.77	11.25
Butyl glycol acetate	204	8.89
Ethyl acetate	97.56	9.09
Dibutyl phthalate	284.35	9.88
Triton X-100	522.96	11.10
Irgasol NA	522.96	11.10

tension of the oil phase decreased by the non-ionic surfactants addition, due to lowered interfacial interactions among the components or the solubility decrease. The Flory-Huggins model based calculations, however, suffer some major deficiencies such as ignoring the compressibility of the components during mixing, which lead to wrong thermodynamic forecast of the mixture in some cases [27].

Typical optical micrograph of the prepared colloidal systems is shown in Figure 6. The number average particle size of the sample is about 15  $\mu$ m. The number average particle size of the crude latex is reduced to 16  $\mu$ m from 35  $\mu$ m, while stayed almost constant and reduced to 10  $\mu$ m by an oil phase BGA content increases from 50% to 62.5%, 75% and 87.5%, respectively. The BGA content of the oil phase

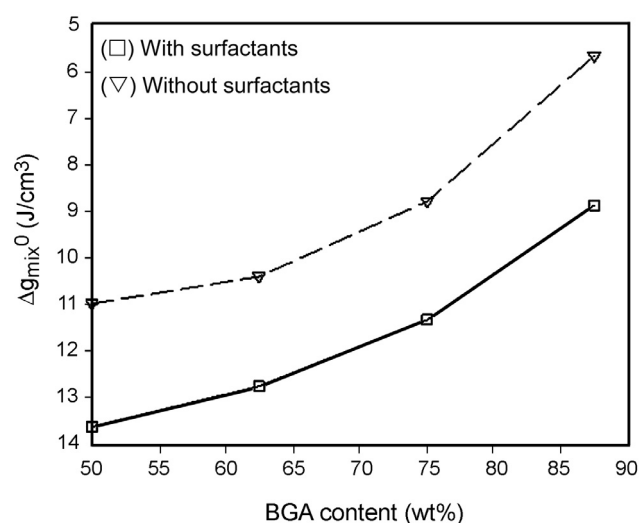


**Figure 5.** Flory-Huggins based calculated free energy density of mixing nitrocellulose solution versus its BGA content (solid and dashed lines are for eye guidance).

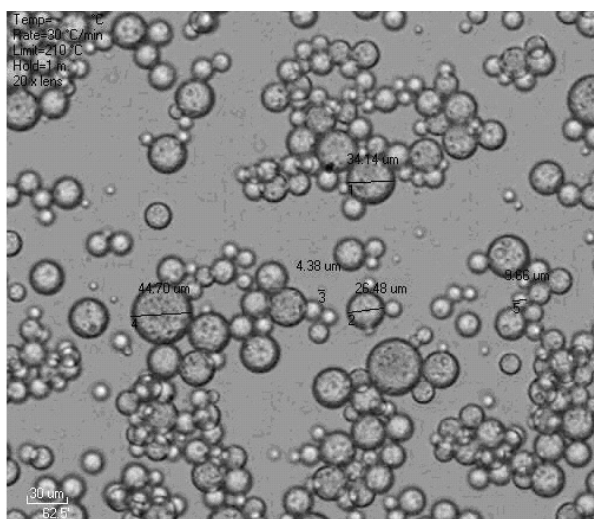


**Figure 6.** Optical micrograph of the nitrocellulose droplets of samples 1-2.

mixed solvents being increased from 50 to 62.5 wt% and then to 75 and 87.5 wt% raised its viscosity by 50 wt%, and afterwards a more severe viscosity jump was observed (Figure 7). Free energy density of mixing of two phases (water and oil) calculated which was based on the Flory-Huggins model also decreased by the increased oil phase BGA content or decreased average particle size (Figure 7). Oil phase viscosity rise might have enhanced droplet break up, which corresponds to lower free energy density of mixing the colloidal components. Turbidity evolution studies of the crude latexes showed delay time decrease from 100 to 57 min by the non-volatile solvent increase up to 75 wt% and led to luminosity plateau (Figure 8). The increase in BGA content of 87.5 wt%, however, rose the delay time to 150 min and luminosity plateau extension to 330 min. In other words, crude latexes stayed stable for some time, delay time, while they started instability via particle settlement leading to colloid luminosity rise. The lower sedimentation rate by increased butyl glycol acetate content was attributed to the smaller droplet size via the oil phase viscosity increase and lower free energy density of mixing two phases. Phenomenologically, sedimentation rate or colloidal average particle size scales oil phase viscosity and colloidal mixing free energy density are as follows:

$$\text{Sedimentation rate} \propto \text{particle size} \propto (\Delta g_{\text{mix}}^C)^\alpha \eta^\beta \quad (3)$$

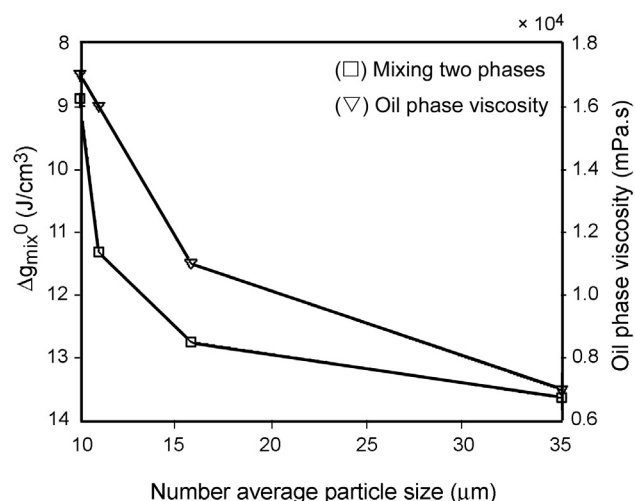


**Figure 7.** Calculated free energy density of mixing two phases and oil phase viscosity versus final number average particle size of the crude latex (solid lines are for eye guidance).

where  $\Delta g_{\text{mix}}^c$  is the free energy density of mixing oil and water phases while  $\eta$  stands for the oil phase viscosity. Plot of the number average particle size versus  $\Delta g_{\text{mix}}^c$  and  $\eta$  was best fitted ( $r^2 = 0.98$ ) with  $\alpha$  and  $\beta$  of 0.09 and -1.31, respectively (Figure 9). In other words, colloid average particle size or sedimentation rate depends weakly on the free energy density of colloid's main components while strong reverse dependence on oil phase viscosity has been inferred.

None of the prepared colloidal systems could be filtered through the polycarbonate membrane under 10 atm of nitrogen pressure. While, direct premix membrane filtration of emulsions with mixed non-ionic and ionic surfactants has not been reported, combination of fatty alcohols along with ionic surfactants [5], anionic [23] or non-ionic surfactants [28] have been practiced. Non-ionic surfactants showed higher dynamic surface tensions in comparison with ionic surfactants leading to less permeation through micron-size porous glass membrane [28]. Non-ionic surfactants also increase water phase viscosity due to their aqueous solubility which facilitates droplet break up process in the membrane pores. They have a long ethoxylated tail which can polarize the non-polar oil phase and make it similar to polycarbonate. Therefore, it may have

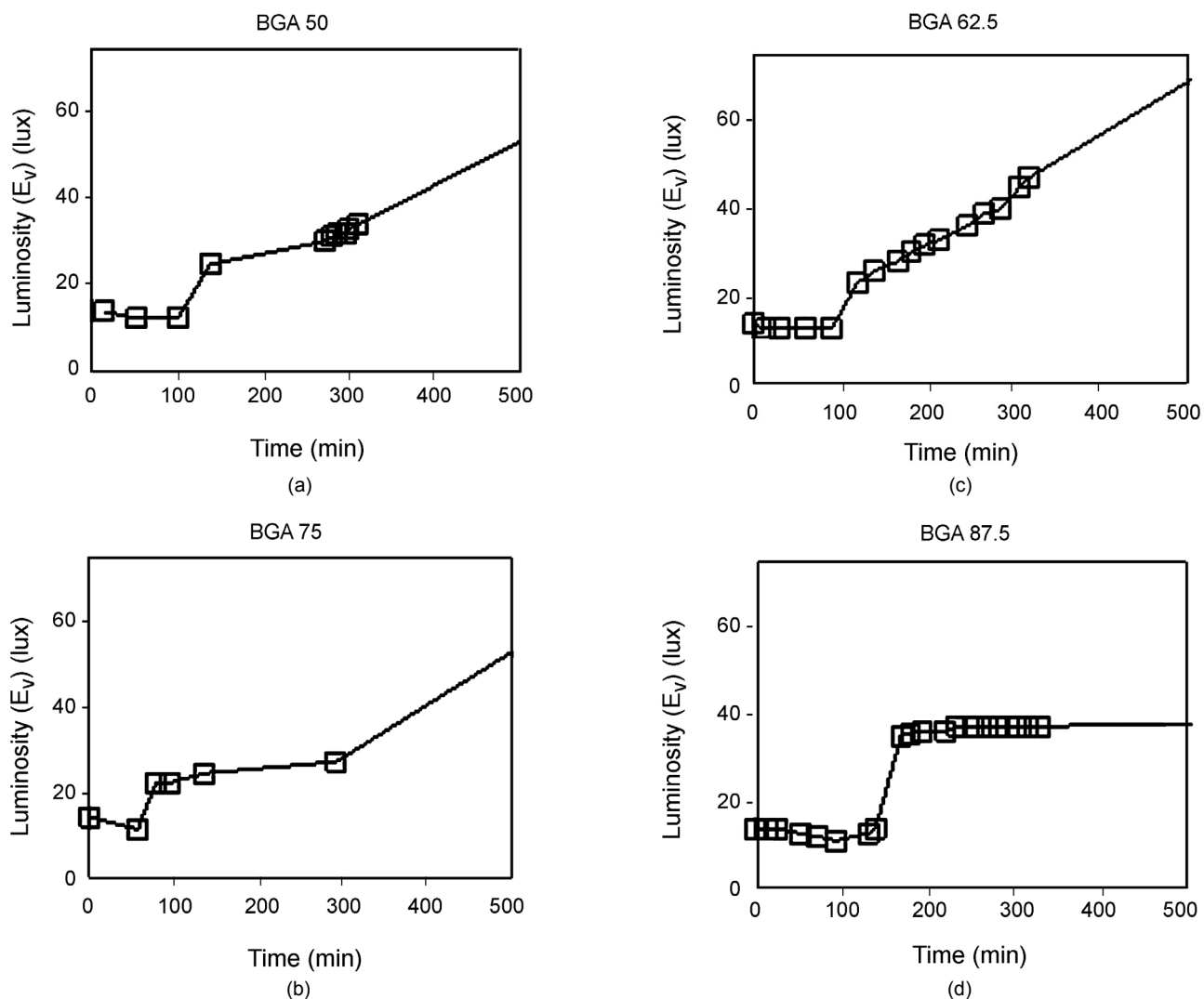


Figure 8. Luminosity of the colloidal system prepared with different BGA contents in their solvent mixture.

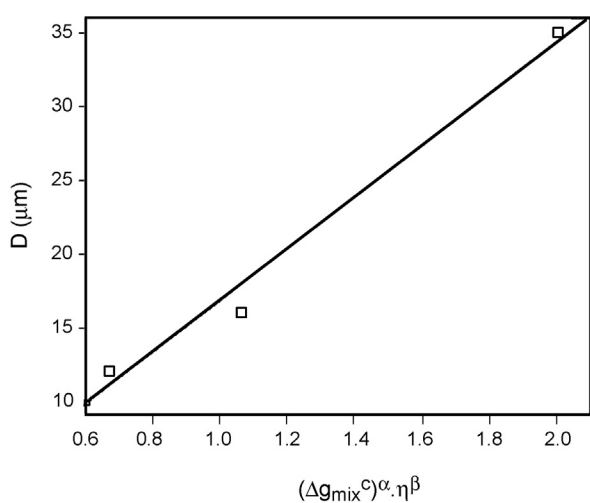


Figure 9. Crude latex number average particle size as a function of  $(\Delta g_{\text{mix}}^c)$  and  $\eta$ .

higher polarity than water and to inverse the emulsion type to W/O during its permeation through polar membrane [20]. In addition, non-ionic surfactants can attach polar membrane surface through their hydrophilic parts leaving their hydrophobic parts into water phase which prevents water permeation through secondary hydrophobe membrane [28,29]. Contact angle of the emulsion drop on membrane was  $15^\circ$  higher than the oil phase drop on polycarbonate membrane.

### CONCLUSION

Turbidity evolution studies of direct emulsified NC solutions in mixed butyl glycol acetate and ethyl

acetate solvents containing two non-ionic surfactants in water phase showed colloidal particle size and lowered sedimentation rate by non-volatile solvent percentage increases. The BGA content increase enhanced the oil phase viscosity and free energy density of mixing of the colloid's main components,  $\Delta g_{\text{mix}}^c$ . The power law dependence of sedimentation rate or average colloidal particle size on  $\Delta g_{\text{mix}}^c$  and  $\eta$  were 0.09 and -1.31, respectively. In other words,  $\Delta g_{\text{mix}}^c$  of two phases and oil phase viscosity increase, showed a mild and severe particle size and sedimentation rate decreases, respectively. Application of non-ionic surfactants suppressed the crude latex micro-filterability due to their long ethoxylated tails, leading to higher dynamic surface tensions and adsorption to the surface of polar polymeric membrane.

## REFERENCES

- Chen CC, Webster JR, Hong RI, Tsi YR, Tseng KY, Chang P, Process for forming nitrocellulose films, *US Patent 7235307 B2* (2007).
- Winchester C, Charles M, Waterborne nitrocellulose wood lacquers with lower VOC, *J Coating Technol*, **63**, 47, 1991.
- Mandal AB, Shape, size, hydration and flow behavior of nitrocellulose lacquer: emulsion in absence and presence of urea, *JAOCS*, **64**, 1202-1207, 1987.
- Lovell PA, El-Aasser MS, *Emulsion Polymerization and Emulsion Polymers*, John Wiley, NY, Chapter 3, 1997.
- Mohammadi N, Kim KD, Sperling LH, Klein A, Direct miniemulsification of anionically synthesized polystyrene to form uniform submicrometer particle, *J Colloid Interface Sci*, **157**, 124-130, 1993.
- Wedlock DJ, *Controlled Particle, Droplet and Bubble Formation*, Butterworth, England, Chs 7-9, 1994.
- Wiering JA, Van Dieren F, Janssen JJM, Agterof WGM, Droplet breakup mechanisms during emulsification in colloid mills at high dispersed phase volume fraction, *Chem Eng Res Dev*, **74**, 554-562, 1996.
- Giribabu K, Ghosh P, Adsorption of nonionic surfactants at fluid-fluid interfaces: importance in the coalescence of bubbles and drops, *Chem Eng Sci*, **62**, 3057-3067, 2007.
- Dale PJ, Kijlstra J, Vincent B, The temperature stability of single and mixed emulsions stabilized by non-ionic surfactants, *Colloid Surface A: Physicochem Eng Aspects*, **291**, 85-92, 2006.
- Sanfeld A, Steinchen A, Emulsions stability, from dilute to dense emulsions - role of drops deformation, *Adv Colloid Interface Sci*, **140**, 1-65, 2008.
- Alexander F, El-Aasser MS, Process model for latex film formation: optical clarity fronts, *J Coating Technol*, **73**, 41-48, 2001.
- Akiba I, Masunaga H, Sasaki K, Jeong Y, Sakurai K, Phase behavior of hydrogen-bonded polymer-surfactant mixtures in selective solvent, *Macromolecules*, **37**, 10047-10051, 2004.
- Feng S, Xiong X, Zhang G, Xia N, Chend Y, Wang W, Hierarchical structure in oriented fibers of a dendronized polymer, *Macromolecules*, **42**, 281-287, 2009.
- Baloch MK, Ahmad F, Rauf A, Durrani GF, Effect of polyethyleneoxide and sodium chloride over the micellization of SLS, *J Appl Polym Sci*, **114**, 1444-1448, 2009.
- Huibers PDT, Shah DO, Evidence for synergism in non-ionic surfactant mixtures: enhancement of solubilization in water-in-oil microemulsions, *Langmuir*, **13**, 5762-5765, 1997.
- Johnson KA, Shah DO, Effect of oil chain length and electrolytes on water solubilization in alcohol-free pharmaceutical microemulsions, *J Colloid Interf Sci*, **107**, 269-271, 1985.
- Nickel D, Nitsch C, Kurzendorfer P, Yon Rybinski W, Interfacial properties of surfactant mixtures with alkyl polyglycosides, *Prog Colloid Polym Sci*, **89**, 249-252, 1992.
- Nakashima T, Shimizu M, Kukizaki M, Membrane emulsification by microporous glass, *Key Eng Mater*, **61**, 513-516, 1991.
- Jeong P, Dimonie VL, Daniels ES, El-Aasser MS, Direct miniemulsification of Kraton rubber/styrene solution. I. Effect of Manton-Gaulin homogenizer, sonifier, and membrane filtration, *J Appl Polym Sci*, **89**, 451-464, 2003.
- Vladisavljevic GT, Shimizu M, Nakashima T,

- Preparation of monodisperse multiple emulsions at high production rates by multi-stage premix membrane emulsification, *J Memb. Sci*, **244**, 97-106, 2004.
21. Lobo A, Cambiella A, Benito JM, Pazos C, Coca J, Ultrafiltration of oil-in-water emulsions with ceramic membranes: influence of pH and cross-flow velocity, *J Membr Sci*, **278**, 328-334, 2006.
  22. Hollabaugh CB, Nitrocellulose emulsion, *US Patent 2101066* (1937).
  23. Becher P, *Encyclopedia of Emulsion Technology* (1), Marcel & Dekker, NY, Chs 2-5, 1988.
  24. Vladisavljevic GT, Surh G, McClements JD, Effect of emulsifier type on droplet disruption in repeated shirasu porous glass membrane homogenization, *Langmuir*, **22**, 4526-4533, 2006.
  25. Carr C, Wallstom E, Theoretical aspects of self-stratification, *Prog Org Coat*, **28**, 161-171, 1996.
  26. Daoud M, Cotton JP, Farnoux B, Jannink G, Sarma G, Benoit H, Duplessix R, Picot C, De Gennes PG, Solutions of flexible polymers, neutron experiments and interpretation, *Macromolecules*, **8**, 804-818, 1975.
  27. Ruzette AVG, Mayes AM, A simple free energy model for weakly interacting polymer blends, *Macromolecules*, **34**, 1894-1907, 2001.
  28. Liu C, Caothien S, Hayes J, Caothuy T, Otoyoy T, Ogawa T, Membrane Chemical Cleaning: From Art to Science, Pall Corporation, Port Washington, NY 11050, USA, [http://www.pall.com/water\\_19565.asp](http://www.pall.com/water_19565.asp), available in 30 December, 15, 2008.
  29. Paul JH, Jeffrey WH, The effect of surfactants on the attachment of estuarine and marine bacteria to surfaces, *Can J Microbiol*, **31**, 224-228, 1984.